

EPR pairing dynamics in Hubbard model with resonant U

X. Z. Zhang^{1,2} and Z. Song^{1,*}

¹*School of Physics, Nankai University, Tianjin 300071, China*

²*College of Physics and Materials Science, Tianjin Normal University, Tianjin 300387, China*

We study the dynamics of the collision between two fermions in Hubbard model with on-site interaction strength U . The exact solution shows that the scattering matrix for two-wavepacket collision is separable into two independent parts, operating on spatial and spin degrees of freedom, respectively. The S-matrix for spin configuration is equivalent to that of Heisenberg-type pulsed interaction with the strength depending on U and relative group velocity v_r . This can be applied to create distant EPR pair, through a collision process for two fermions with opposite spins in the case of $|v_r/U| = 1$, without the need for temporal control and measurement process. Multiple collision process for many particles is also discussed.

PACS numbers: 03.65.-w, 11.30.Er, 75.10.Jm, 64.70.Tg

I. INTRODUCTION

Pairing is the origin of many fascinating phenomena in nature, ranging from superconductivity to quantum teleportation. Owing to the rapid advance of experimental techniques, it has been possible both to produce Cooper pairs of fermionic atoms and to observe the crossover between a Bose-Einstein condensate and a Bardeen-Cooper-Schrieffer superfluid [1–3]. The dynamic process of pair formation is of interest in both condensed matter physics and quantum information science. On one hand, the collective behavior of pairs gives rise to macroscopic properties in many-body physics. On the other hand, a single entangled pair is a promising quantum information resource for future quantum computation.

In recent years, the controlled setting of ultracold fermionic atoms in optical lattices is regarded as a promising route to enabled quantitative experimental tests of theories of strongly interacting fermions [4–7]. In particular, fermions trapped in optical lattices can directly simulate the physics of electrons in a crystalline solid, shedding light on novel physical phenomena in materials with strong electron correlations [4, 8, 9]. A major effort is devoted to simulate the Fermi-Hubbard model by using ultracold neutral atoms [10–12]. This approach offers experimental access to a clean and highly flexible Fermi-Hubbard model with a unique set of observables [13] and therefore, motivate a large number of works on Mott insulator phase [14, 15] and transport properties [16, 17], stimulating further theoretical and experimental investigations on the dynamics of strongly interacting particles for the Fermi Hubbard model.

In this paper, we study the dynamics of the collision between two fermions with various spin configurations. The particle-particle interaction is described by Hubbard model, which operates spatial and spin degrees of freedom in a mixed manner. Based on the Bethe ansatz

solution, the time evolution of two fermionic wave packets with identical size is analytically obtained. We find that the scattering matrix of the collision is separable into two independent parts, operating on spatial and spin degrees of freedom, respectively. The scattered two particles exhibit dual features. The spatial part behaves as classical particles, swapping the momenta, while the spin part obeys the isotropic Heisenberg-type exchange coupling. The coupling strength depends on the Hubbard on-site interaction and relative group velocity of two wavepackets. This finding can be applied to create distant EPR pair, through a collision process for two fermions with opposite spins without the need for temporal control and measurement process. Multiple collision process for many particles is also discussed.

The paper is organized as follow. In Sec. II, we present the model Hamiltonian and analyze the symmetries. In Sec. III, we investigate some exact results obtained by Bethe ansatz concerning the two-particle problem. In Sec. IV, we explore the dynamics of wavepacket collision. Sec. V is devoted to construct the scattering matrix for the collision process and the corresponding equivalent Hamiltonian. In Sec. VI, we apply two-particle S-matrix to the case of multi-fermion collision. Finally, we give a summary and discussion in Sec. VII.

II. MODEL HAMILTONIANS AND SYMMETRIES

A one-dimensional Hubbard Hamiltonian on an N -site ring reads

$$H = -\kappa \sum_{i=1, \sigma=\uparrow\downarrow}^N \left(c_{i, \sigma}^\dagger c_{i+1, \sigma} + \text{H.c.} \right) + U \sum_i n_{i\uparrow} n_{i\downarrow}, \quad (1)$$

where $c_{i, \sigma}^\dagger$ is the creation operator of the fermion at the site i with spin $\sigma = \uparrow, \downarrow$ and U is the on-site interaction. The tunneling strength and the on-site interaction between bosons are denoted by κ and U . For the sake of clarity and simplicity, we only consider odd-site sys-

* songtc@nankai.edu.cn

tem with $N = 2N_0 + 1$, and periodic boundary condition $c_{i,\sigma} = c_{i+N,\sigma}$.

We analyze three symmetries of the Hamiltonian as following, which is critical for achieving a two-particle solution. The first is particle-number conservation $[N_\sigma, H] = 0$, where $N_\sigma = \sum_i c_{i,\sigma}^\dagger c_{i,\sigma}$, which ensures that one can solve the eigen problem in the invariant subspace with fixed N_σ , no matter U is real or complex. The second is the translational symmetry, $[T_1, H] = 0$, where T_1 is the shift operator defined as

$$\begin{aligned} T_1^{-1} c_{i,\sigma}^\dagger T_1 &= c_{i+1,\sigma}^\dagger, \\ \text{or } T_1^{-1} c_{k,\sigma}^\dagger T_1 &= e^{-ik} c_{k,\sigma}^\dagger, \end{aligned} \quad (2)$$

with

$$\begin{aligned} c_{k,\sigma}^\dagger &= \frac{1}{\sqrt{N}} \sum_j e^{ikj} c_{j,\sigma}^\dagger, \\ k &= 2n\pi/N, n \in [1, N]. \end{aligned} \quad (3)$$

This allows invariant subspace spanned by the eigenvector of operator T_1 . Based on this fact, one can reduce the two-particle problem to a single-particle problem. The final is the SU(2) symmetry, $[S^{\pm,z}, H] = 0$ and $[S^2, H] = 0$, where the spin operators are defined as

$$S^+ = (S^-)^\dagger = \sum_i c_{i,\uparrow}^\dagger c_{i,\downarrow}, \quad (4)$$

$$S^z = \frac{1}{2} \sum_i \left(c_{i,\uparrow}^\dagger c_{i,\uparrow} - c_{i,\downarrow}^\dagger c_{i,\downarrow} \right), \quad (5)$$

which satisfy the relation $[S^+, S^-] = 2S^z$.

Now based on the above analysis, we construct the basis of the two-fermion invariant subspace as following

$$|\phi_0^-(K)\rangle = \frac{1}{\sqrt{N}} \sum_j e^{iKj} c_{j,\uparrow}^\dagger c_{j,\downarrow}^\dagger |\text{vac}\rangle, \quad (6)$$

$$\begin{aligned} |\phi_r^\pm(K)\rangle &= \frac{1}{\sqrt{2N}} e^{iKr/2} \sum_j e^{iKj} \\ &\times \left(c_{j,\uparrow}^\dagger c_{j+r,\downarrow}^\dagger \pm c_{j,\downarrow}^\dagger c_{j+r,\uparrow}^\dagger \right) |\text{vac}\rangle, \quad (r > 1), \end{aligned}$$

and

$$\frac{S^\pm}{\sqrt{2}} |\phi_r^\pm(K)\rangle = \frac{1}{\sqrt{N}} e^{iKr/2} \sum_j e^{iKj} c_{j,\pm\uparrow}^\dagger c_{j+r,\pm\uparrow}^\dagger, \quad (r > 1), \quad (7)$$

where K is the momentum vector, indexing the subspace. These bases are eigenvectors of the operators N_σ , T_1 , S^2 and S^z . Straightforward algebra yields

$$N_\sigma |\phi_0^-(K)\rangle = |\phi_0^-(K)\rangle, \quad (8)$$

$$N_\sigma |\phi_r^\pm(K)\rangle = |\phi_r^\pm(K)\rangle, \quad (9)$$

$$N_\uparrow \frac{S^\pm}{\sqrt{2}} |\phi_r^\pm(K)\rangle = (1 \pm 1) \frac{S^\pm}{\sqrt{2}} |\phi_r^\pm(K)\rangle, \quad (10)$$

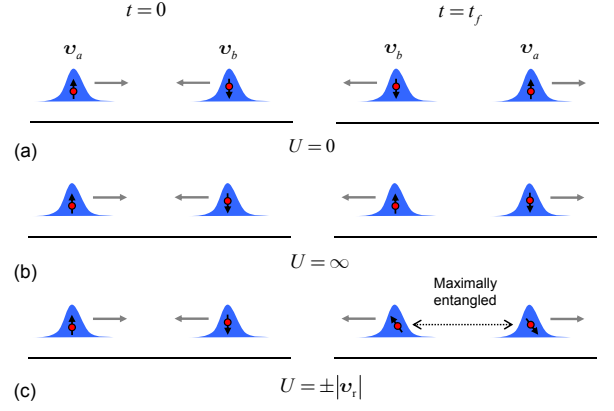


FIG. 1. (Color online) Schematic illustration of the collision process of two separated fermionic wavepackets with opposite spin orientations for three typical values of U . In all cases, the collisions result in momentum swap, but different spin configurations: (a) $U = 0$, swap; (b) $U = \infty$, unchange; (c) $U = \pm |v_r|$, maximal entanglement.

and

$$T_1 |\phi_0^-(K)\rangle = e^{-iKj} |\phi_0^-(K)\rangle, \quad (11)$$

$$T_1 |\phi_r^\pm(K)\rangle = e^{-iKj} |\phi_r^\pm(K)\rangle, \quad (12)$$

$$T_1 S^\pm |\phi_r^\pm(K)\rangle = e^{-iKj} S^\pm |\phi_r^\pm(K)\rangle, \quad (13)$$

while

$$S^2 |\phi_0^-(K)\rangle = S^2 |\phi_r^-(K)\rangle = 0, \quad (14)$$

$$S^2 |\phi_r^+(K)\rangle = 2 |\phi_r^+(K)\rangle, \quad (15)$$

$$S^2 S^\pm |\phi_r^\pm(K)\rangle = 2 S^\pm |\phi_r^\pm(K)\rangle, \quad (16)$$

and

$$S^z |\phi_0^-(K)\rangle = S^z |\phi_r^\pm(K)\rangle = 0, \quad (17)$$

$$S^z S^\pm |\phi_r^\pm(K)\rangle = \pm S^\pm |\phi_r^\pm(K)\rangle. \quad (18)$$

Then there are four invariant subspaces with $(S, S^z) = (0, 0)$, $(1, 0)$, and $(1, \pm 1)$ involved.

III. TWO-PARTICLE SOLUTIONS

Now we look at the two-particle solution in each invariant subspace. We only focus on the solutions in subspaces $(0, 0)$ and $(1, 0)$, since the one in subspace $(1, \pm 1)$ can be obtained directly from that in subspace $(1, 0)$ by operator S^\pm . A two-particle state can be written as

$$|\varphi_K^\pm\rangle = \sum_r f_{K,k}^\pm(r) |\phi_r^\pm(K)\rangle, \quad \left(f_K^+(0) = f_{K,k}^-(1) = 0 \right), \quad (19)$$

where the wave function $f_{K,k}^\pm(r)$ satisfies the Schrödinger equations

$$\begin{aligned} Q_r^K f_{K,k}^+(r+1) + Q_{r-1}^K f_{K,k}^+(r-1) + \\ [(-1)^n Q_r^K \delta_{r,N_0} - \varepsilon_K] f_{K,k}^+(r) = 0, \end{aligned} \quad (20)$$

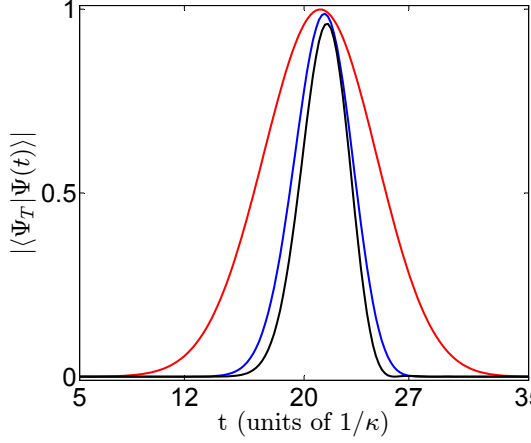


FIG. 2. (Color online) Plots of the fidelity $|\langle \Psi_T | \Psi(t) \rangle|$ with the parameters $N_a = 20, N_b = 62, k_a = -k_b = \pi/2$, in the system Eq. (1) with $N = 81$ and $U = v_r$. The red, blue and black lines represent the plots of fidelity $|\langle \Psi_T | \Psi(t) \rangle|$ in the condition of $\alpha = 0.13, 0.26$, and 0.33 , respectively. It shows that the fidelity is close 1, as α approaches to 0, which accords with the theoretical analysis in the text.

and

$$Q_r^K f_{K,k}^-(r+1) + Q_{r-1}^K f_{K,k}^-(r-1) + [U\delta_{r,0} + (-1)^n Q_r^K \delta_{r,N_0} - \varepsilon_K] f_{K,k}^-(r) = 0, \quad (21)$$

with the eigen energy ε_K in the invariant subspace indexed by K . Here factor $Q_r^K = -2\sqrt{2}\kappa \cos(K/2)$ for $r = 0$ and $-2\kappa \cos(K/2)$ for $r \neq 0$, respectively. As pointed in Ref. [18] in previous works, the eigen problem of two-particle matrix can be reduced to the that of single particle. We see that the solution of (21) is equivalent to that of the single-particle $N_0 + 1$ -site tight-binding chain system with nearest-neighbour (NN) hopping amplitude Q_j^K , on-site potentials U and $(-1)^{n+1} 2\kappa \cos(K/2)$ at 0th and N_0 th sites, respectively. The solution of (20) corresponds to the same chain with infinite U . In this work, we only concern the scattering solution by the 0th end. In this sense, f_K^- can be obtained from the equivalent Hamiltonian

$$H_{\text{eq}}^K = U |0\rangle \langle 0| + \sum_{i=1}^{\infty} (Q_i^K |i\rangle \langle i+1| + \text{H.c.}). \quad (22)$$

Based on the Bethe ansatz technique, the scattering solution can be expressed as

$$f_{K,k}^-(j) = e^{-ikj} + R_{K,k} e^{ikj}, \quad (23)$$

with eigen energy $\varepsilon_K(k) = -4\kappa \cos(K/2) \cos k$, $k \in [0, \pi]$. Here the reflection amplitude

$$R_{K,k} = \frac{i\lambda_{K,k} + U}{i\lambda_{K,k} - U} = e^{i\Delta}, \quad (24)$$

where

$$\lambda_{K,k} = 4\kappa \cos(K/2) \sin k, \quad (25)$$

$$\Delta = 2 \tan^{-1} \left(-\frac{U}{\lambda_{K,k}} \right). \quad (26)$$

And $f_{K,k}^+$ can be obtained from $f_{K,k}^-$ by taking $U = \infty$. We note that $R_{K,k}(-U) = R_{K,k}^* = R_{K,-k}$, which reveals a dynamic symmetry of the Hubbard model with respect to the sign of U .

IV. DYNAMICS OF WAVEPACKET COLLISION

In this section, we investigate the dynamics of two-wavepackets collision based on the above formalism. We begin with our investigation from the time evolution of an initial state

$$|\Phi\rangle = |\Phi_{a,\sigma}\rangle |\Phi_{b,\sigma'}\rangle, \quad (27)$$

which represents two separable fermions a and b , with spin σ and σ' , respectively. Here

$$|\Phi_{\gamma,\sigma}\rangle = \frac{1}{\sqrt{\Omega}} \sum_j e^{-\alpha^2(j-N_\gamma)^2} e^{ik_\gamma j} c_{j,\sigma}^\dagger |\text{Vac}\rangle, \quad (28)$$

with $\gamma = a, b$ and $N_a - N_b \gg 1/\alpha$, is a wavepacket with a width $2\sqrt{\ln 2}/\alpha$, a central position N_γ and a group velocity $v_\gamma = -2\kappa \sin k_\gamma$. We focus on the case $(\sigma, \sigma') = (\uparrow, \downarrow)$. The obtained result can be extended to other cases. In order to calculate the time evolution of state $|\Phi\rangle$, two steps are necessary. At first, the projection of $|\Phi\rangle$ on the basis sets $\{|\phi_r^+(K)\rangle\}$ and $\{|\phi_r^-(K)\rangle\}$ can be given by the decomposition

$$2|\Phi_{a,\uparrow}\rangle |\Phi_{b,\downarrow}\rangle = (|\Phi_{a,\uparrow}\rangle |\Phi_{b,\downarrow}\rangle + |\Phi_{a,\downarrow}\rangle |\Phi_{b,\uparrow}\rangle) + (|\Phi_{a,\uparrow}\rangle |\Phi_{b,\downarrow}\rangle - |\Phi_{a,\downarrow}\rangle |\Phi_{b,\uparrow}\rangle). \quad (29)$$

Secondly, introducing the transformation

$$N_c = \frac{1}{2}(N_a + N_b), r_c = N_b - N_a, \quad (30)$$

$$k_c = \frac{1}{2}(k_a + k_b), q_c = k_b - k_a, \quad (31)$$

$$l = j + r, \quad (32)$$

and using the identities

$$\begin{aligned} & 2 \left[(j - N_a)^2 + (l - N_b)^2 \right] \\ &= [(j+l) - (N_a + N_b)]^2 + [(l-j) - (N_b - N_a)]^2 \\ & 2(k_a j + k_b l) \\ &= (k_a + k_b)(j+l) + (k_b - k_a)(l-j), \end{aligned} \quad (33)$$

we have

$$\begin{aligned} & \frac{1}{\sqrt{2}} (|\Phi_{a,\uparrow}\rangle |\Phi_{b,\downarrow}\rangle \pm |\Phi_{a,\downarrow}\rangle |\Phi_{b,\uparrow}\rangle) \\ &= \frac{1}{\sqrt{\Omega_1}} \sum_K e^{-(K-2k_c)^2/4\alpha^2} \\ & \times e^{-iN_c(K-2k_c)} |\psi_K^\pm(r_c, q_c)\rangle, \end{aligned} \quad (35)$$

with

$$|\psi_K^\pm\rangle = \frac{1}{\sqrt{\Omega_2}} \sum_r e^{-\alpha^2(r-r_c)^2/2} e^{iq_c r/2} |\phi_r^\pm(K)\rangle, \quad (36)$$

where $\Omega_{1,2}$ is the normalized factor.

We note that the component of state $|\Phi\rangle$ on each invariant subspace indexed by K represents an incident wavepacket along the chain described by H_{eff}^K . This wavepacket has width $2\sqrt{\ln 2}/\alpha$, central position $r_c = N_b - N_a$ and group velocity $v = -4\kappa \cos(K/2) \sin(q_c/2)$. Accordingly, the time evolution of state $|\Phi\rangle$ can be derived by the dynamics of each sub wavepacket in each chain H_{eff}^K , which eventually can be obtained from Eq. (23). According to the solution, the evolved state of $|\psi_K^\pm(r_c, q_c)\rangle$ can be expressed approximately in the form $e^{i\beta(r'_c)} R_{2k_c, q_c/2} |\psi_K^\pm(r'_c, -q_c)\rangle$, which represents a reflected wavepacket. Here $\beta(r'_c)$ is an overall phase, as a function of r'_c , the position of the reflected wavepacket, being independent of U . In addition, it is easy to check out that, in the case with $\alpha \ll 1$, the initial state distribute mainly in the invariant subspace $K = 2k_c$, where the wavepacket moves with the group velocity $v_r = -4\kappa \cos(k_c) \sin(q_c/2) = v_b - v_a$. Then the state after collision has the approximate form

$$\begin{aligned} |\Phi(\infty)\rangle &= \frac{1 - R_{2k_c, q_c/2}}{\sqrt{\Omega}} \left(\sum_j e^{-\alpha^2(j-N'_a)^2} e^{ik_b j} c_{j,\uparrow}^\dagger |\text{Vac}\rangle \right) \\ &\quad \left(\sum_l e^{-\alpha^2(l-N'_b)^2} e^{ika_l} c_{l,\downarrow}^\dagger |\text{Vac}\rangle \right) \\ &\quad + \frac{1 + R_{2k_c, q_c/2}}{\sqrt{\Omega}} \left(\sum_j e^{-\alpha^2(j-N'_a)^2} e^{ik_b j} c_{j,\downarrow}^\dagger |\text{Vac}\rangle \right) \\ &\quad \left(\sum_l e^{-\alpha^2(l-N'_b)^2} e^{ika_l} c_{l,\uparrow}^\dagger |\text{Vac}\rangle \right), \end{aligned} \quad (37)$$

which also represents two separable wavepackets at N'_a and N'_b respectively. Here Ω is the normalized factor and an overall phase is neglected. We would like to point that the obtained conclusion is based on the fact that the shapes of two wavepackets $|\Phi_{a,\sigma}\rangle$ and $|\Phi_{b,\sigma'}\rangle$ are identical.

V. EQUIVALENT HEISENBERG COUPLING

Now we try to express the two-fermion collision in a more compact form. We will employ an S-matrix to relate the asymptotic spin states of the incoming to outgoing particles. We denote an incident single-particle wavepacket as the form of $|\lambda, p, \sigma\rangle$, where $\lambda = \text{L, R}$ indicates the particle in the left and right of the collision zone, p the momentum, and $\sigma = \uparrow, \downarrow$ the spin degree of freedom. In this context, we give the asymptotic expression for the collision process as

$$|\text{L}, p, \sigma_{\text{L}}\rangle |\text{R}, q, \sigma_{\text{R}}\rangle \mapsto \mathcal{S} |\text{L}, q, \sigma_{\text{L}}\rangle |\text{R}, p, \sigma_{\text{R}}\rangle, \quad (38)$$

where the S-matrix

$$\mathcal{S} = e^{-i(\theta-\pi)(\vec{s}_{\text{L}} \cdot \vec{s}_{\text{R}} - 1/4)}, \quad (39)$$

governs the spin part of the wave function. Here $\vec{s}_{\text{L,R}}$ denotes spin operator for the spins of particles at left or right, $\theta = 2 \tan^{-1} [U / (v_{\text{R}} - v_{\text{L}})]$, where v_{L} and v_{R} represent the group velocity of the left and right wavepacket, respectively. Together with the scattering matrix \mathcal{M} for spatial degree of freedom

$$\mathcal{M} |\text{L}, p, \sigma_{\text{L}}\rangle |\text{R}, q, \sigma_{\text{R}}\rangle = |\text{L}, q, \sigma_{\text{L}}\rangle |\text{R}, p, \sigma_{\text{R}}\rangle, \quad (40)$$

we have a compact expression

$$|f\rangle = \mathcal{M} \mathcal{S} |i\rangle, \quad (41)$$

to connect the initial and final states. In general the total scattering matrix has the form $\exp[-i \int_{-\infty}^{\infty} H dt]$, which is not separable into spatial and spin parts. Then Eq. (41) is only available for some specific initial states, e.g., spatially separable two-particle wavepackets with identical size. This may lead to some interesting phenomena.

It is interesting to note that the scattering matrix for spin is equivalent to the propagator

$$\mathcal{S} = \mathcal{T} \exp \left[-i \int_{-\infty}^{\infty} h(t) dt \right], \quad (42)$$

for a pulsed Hensenberg model with Hamiltonian

$$h(t) = J(t) (\vec{s}_{\text{L}} \cdot \vec{s}_{\text{R}} - 1/4), \quad (43)$$

with $\int J(t) dt = \theta - \pi$. Here \mathcal{T} is time-ordered operator, which can be ignored since only the coupling strength $J(t)$ is time dependent. This observation accords with the fact that, in the large positive U case, the Hubbard model scales on the $t - J$ model [20, 21], which also includes the NN interaction term of isotropic Heisenberg type.

This also indicates that the effect of collision on two spins is equivalent to that of time evolution operation under the Hamiltonian $\vec{s}_{\text{L}} \cdot \vec{s}_{\text{R}}$ at an appropriate instant. In this sense, the collision process can be utilized to implement two-qubit gate. For two coupled-qubit system, the time evolution operator is simply given by

$$\mathcal{U}(t) = \exp(-i \vec{s}_{\text{L}} \cdot \vec{s}_{\text{R}} t), \quad (44)$$

yielding

$$\mathcal{U}(t) |\uparrow\rangle_{\text{L}} |\downarrow\rangle_{\text{R}} = e^{it/4} (\cos \frac{t}{2} |\uparrow\rangle_{\text{L}} |\downarrow\rangle_{\text{R}} - i \sin \frac{t}{2} |\downarrow\rangle_{\text{L}} |\uparrow\rangle_{\text{R}}), \quad (45)$$

where $|\sigma = \uparrow, \downarrow\rangle_{\text{L,R}}$ denotes qubit state. We can see that at instants $t = \pi/2$ and π , the evolved states become

$$\mathcal{U}(\pi/2) |\uparrow\rangle_{\text{L}} |\downarrow\rangle_{\text{R}} = \frac{e^{i\pi/8}}{\sqrt{2}} (|\uparrow\rangle_{\text{L}} |\downarrow\rangle_{\text{R}} - i |\downarrow\rangle_{\text{L}} |\uparrow\rangle_{\text{R}}), \quad (46)$$

$$\mathcal{U}(\pi) |\uparrow\rangle_{\text{L}} |\downarrow\rangle_{\text{R}} = e^{-i\pi/4} |\downarrow\rangle_{\text{L}} |\uparrow\rangle_{\text{R}}, \quad (47)$$

which indicates that $U(\pi/2)$ and $U(\pi)$ are entangling and swap operators, respectively. In practice, such protocols require exact time control of the operation.

Comparing operator $U(t)$ and the S-matrix in Eq. (39), we find that two-qubit operations can be performed by the collision process, where U and relative group velocity $v_r = v_L - v_R$ are connected to the evolution time by the relation

$$t = \theta - \pi = 2 \cot^{-1} \left(\frac{U}{v_r} \right). \quad (48)$$

Then we can implement entangling and swap gates for two flying qubits via dynamic process. To demonstrate the result, we consider several typical cases with $U = 0, \infty$, and $\pm|v_r|$, which correspond to the operations of swap, standby, and entanglement, respectively. The collision processes are illustrated schematically in Fig. 1. The advantage of such a scheme is that the temporal control is replaced by pre-engineered on-state interaction U .

In order to check the above conclusion, numerical simulation is performed. We define the initial and target states as

$$|\Psi(0)\rangle = |L, p, \uparrow\rangle |R, q, \downarrow\rangle, \quad (49)$$

$$|\Psi_T\rangle = e^{i\frac{\theta}{2}} (-i \sin \frac{\theta}{2} |L, q, \uparrow\rangle |R, p, \downarrow\rangle + \cos \frac{\theta}{2} |L, q, \downarrow\rangle |R, p, \uparrow\rangle), \quad (50)$$

where $|\Psi_T\rangle$ possess the same relative position but the exchanged momentum compared with the state $|\Psi(0)\rangle$ as in Eq. (49). On the other hand, we consider the evolved state $|\Psi(t)\rangle$ for the initial state being $|\Psi(0)\rangle$ driven by the Hamiltonian (1), and calculate the fidelity $|\langle \Psi_T | \Psi(t) \rangle|$ in Fig. 2. It is shown that when the state $|\Psi(0)\rangle$ evolves to the same position with $|\Psi_T\rangle$, the fidelity $|\langle \Psi_T | \Psi(t) \rangle|$ is almost to 0, which is in agreement with our previous theoretical analysis.

VI. MULTIPLE COLLISION

We apply our result to many-body system. Considering the case that the initial state is consisted of many separable local particles with the same group velocity, termed as many-particle wavepacket train (MPWT), our result can be applicable if each collision time is exact known. In this paper, we only demonstrate this by a simple example. We consider the collision of two MPWTs with particle numbers M and N ($N \geq M$). All the distances between two adjacent particles in two trains are identical. The initial state is

$$\prod_{m=1}^M |L_m, p, \sigma_m\rangle \prod_{n=1}^N |R_n, q, \tau_n\rangle, \quad (51)$$

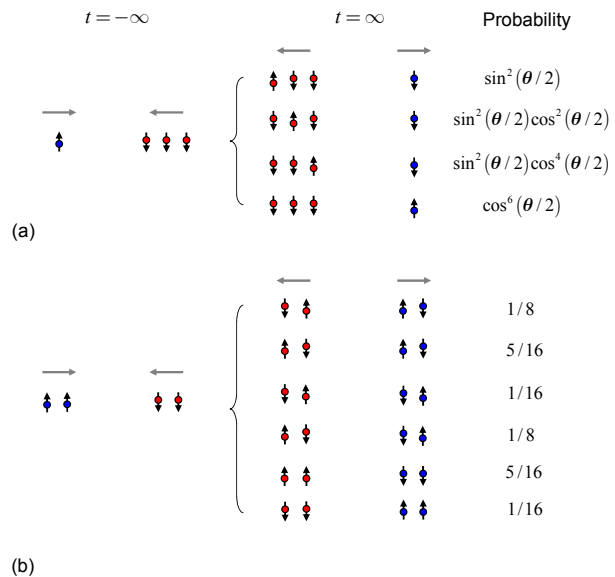


FIG. 3. (Color online) Schematic illustration of the collision between the two MPWTs. (a) An incident single fermion comes from the left denoted as blue spin and collides with 3-fermion train, which comes from the right denoted as red spins. It can be seen that the single fermion keep the original momentum, but it entangles with the 3-fermion train at the end of the collision. The amplitudes of the four states are listed. It is shown that the final state is direct product between the states of single fermion and 3-fermion train when $\theta = \pi$, $\theta = 0$ with the corresponding parameter $U = \infty, 0$, respectively. (b) The collision between the two MPWTs come from the opposite direction with particle number $N = 2$. And the probability for the superposition of states is listed with $\theta = \pi/2$.

where $\{L_m\}$ and $\{R_n\}$ denote the sequences of particles, $\{\sigma_m\}$ and $\{\tau_n\}$ denote the spin configurations in each trains. According to the above analysis, after collisions the final state has the form of

$$\prod_{m=1}^M |L_m, q, \sigma'_m\rangle \prod_{n=1}^N |R_n, p, \tau'_n\rangle, \quad (52)$$

where the spin configurations $\{\sigma'_m\}$ and $\{\tau'_n\}$ are determined by the S-matrix, which is the time-ordered product of all two-particle S-matrices. During the collision process, the positions of particles in each train are always spaced by equal intervals. This makes it easier to determine the times of each collisions. Then the final state can be written as

$$\prod_{l=1}^M S_l \prod_{n=1}^N |L_n, q, \tau_n\rangle \prod_{m=1}^M |R_m, p, \sigma_m\rangle, \quad (53)$$

where

$$S_l = \prod_{n=1}^N s_{l, N-n+1}, \quad (54)$$

and

$$s_{jk} = e^{-i(\theta-\pi)(\vec{\tau}_j \cdot \vec{\sigma}_{k-1})/4}, \quad (55)$$

where $\vec{\tau}_j$ and $\vec{\sigma}_k$ are corresponding Pauli matrices. Applying the formula in Eq. (53) to the case with $M = 1$, $\sigma_1 = \uparrow$, $\tau_n = \downarrow$, $n \in [1, N]$, we obtain

$$\begin{aligned} & |L_1, p, \uparrow\rangle \prod_{n=1}^N |R_n, q, \downarrow\rangle \mapsto \\ & -i \sum_{j=1}^N e^{i\frac{\theta}{2}j} \sin \frac{\theta}{2} \cos^{(j-1)} \frac{\theta}{2} \\ & \times \frac{1 + \vec{\sigma}_1 \cdot \vec{\tau}_j}{2} \prod_{n=1}^N |L_n, q, \downarrow\rangle |R_1, p, \uparrow\rangle \\ & + e^{i\frac{\theta}{2}N} \cos^N \frac{\theta}{2} \prod_{n=1}^N |L_n, q, \downarrow\rangle |R_1, p, \uparrow\rangle. \end{aligned} \quad (56)$$

This conclusion is still true for the case with unequal-spaced $\{R_n\}$. For illustration, we sketch the case with $M = 1$, $\sigma_1 = \uparrow$, $N = 3$, $\tau_n = \downarrow$, $n \in [1, 3]$ in Fig. 3(a). One can see that the spin part of the final state is the superposition of the combinations of the four spins.

Now we turn to investigate the entanglement between the single fermion and the MPWT with particle number N . As is well known, the generation and controllability of entanglement between distant quantum states have been at the heart of quantum information processing. Such as the applications in the emerging technologies of quantum computing and quantum cryptography, as well as to realize quantum teleportation experimentally [22, 23]. Moreover, quantum entanglement is typically fragile to practical noise. Every external manipulation inevitably induces noise in the system. This suggests a scheme based on the above mentioned collision process for generating the entanglement between a single fermion and the N -fermion train without the need for the temporal control and measurement process. We note that although the incident single fermion keep the original momentum, it entangles with the N -fermion train after the collision, leading to a deterioration of its purity. To measure the entanglement between the single fermion and the N -fermion train, we calculate the reduced density matrix of the single spin

$$\rho_R(\infty) = \begin{pmatrix} \Lambda & 0 \\ 0 & 1 - \Lambda \end{pmatrix}, \quad (57)$$

where

$$\Lambda = \cos^{2N} \frac{\theta}{2}. \quad (58)$$

Thus the purity of the single fermion can be expressed as

$$P(\infty) = \text{Tr}(\rho_R^2) = 2 \left(\Lambda - \frac{1}{2} \right)^2 + \frac{1}{2}, \quad (59)$$

where $\text{Tr}(\dots)$ denotes the trace on the single fermion. For the case of $\Lambda = 0, 1$, we have $P(\infty) = 1$, which requires $\theta = \pi$, and $\theta = 0$, obtained from interaction parameter $U = \infty$, and 0, respectively. It indicates that the single fermion state and N -fermion train state are not entangled. In contrast, the purity $P(\infty) = 1/2$ at $\Lambda = 1/2$ when

$$\theta = 2 \cos^{-1} \left(2^{-\frac{1}{2N}} \right). \quad (60)$$

It corresponds to a completely mixed state of the outgoing single fermion, or maximal entanglement between the single fermion state and N -fermion train. Together with Eq. (24), we have

$$U = (v_R - v_L) \tan \left[\cos^{-1} \left(2^{-\frac{1}{2N}} \right) \right], \quad (61)$$

which reduces to $U \approx (v_R - v_L) \sqrt{\ln 2} N^{-1/2}$ for large N . This indicates that for large N , one needs to take a small U of order $N^{-1/2}$ to generate the maximal entanglement between the single fermion state and N -fermion train, or result in full decoherence of the single fermion.

In the case of two-train collision, the calculation can still be performed in the similar way. However, it is hard to get analytical result for arbitrary system. Here, we sketch the case with $M = 2$, $\sigma_1 = \sigma_2 = \uparrow$, $N = 2$, $\tau_1 = \tau_2 = \downarrow$, in Fig. 3(b). The probability on each spin configuration is listed as illustration.

VII. SUMMARY

In summary, we presented an analytical study for two-fermion dynamics in Hubbard model. We find that the scattering matrix of two-fermion collision is separable into two independent parts, operating on spatial and spin degrees of freedom, respectively, when two incident wavepackets have identical shapes. For two fermions with opposite spins, the collision process can create a distant EPR pair due to the resonance between the Hubbard interaction strength and the relative group velocity. The advantage of this scheme is without the need of temporal control and measurement process. Since it is now possible to simulate the Hubbard model via cold fermionic atoms in optical lattice, these results can be realized experimentally.

ACKNOWLEDGMENTS

We acknowledge the support of the National Basic Research Program (973 Program) of China under Grant No. 2012CB921900 and the CNSF (Grant No. 11374163). X. Z. Zhang is supported by PhD research startup foundation of Tianjin Normal University under Grant No. 52XB1415.

-
- [1] C. A. Regal, M. Greiner, and D. S. Jin, *Observation of Resonance Condensation of Fermionic Atom Pairs*, Phys. Rev. Lett. **92**, 040403 (2004).
- [2] M. W. Zwierlein, C. A. Stan, C. H. Schunck, S. M. F. Raupach, A. J. Kerman, and W. Ketterle, *Condensation of Pairs of Fermionic Atoms near a Feshbach Resonance*, Phys. Rev. Lett. **92**, 120403 (2004).
- [3] T. Bourdel, Khaykovich, J. Cubizolles, J. Zhang, F. Chevy, M. Teichmann, L. Tarruell, S. J. J. M. F. Kokkelmans, and C. Salomon, *Experimental Study of the BEC-BCS Crossover Region in Lithium 6*, Phys. Rev. Lett. **93**, 050401 (2004).
- [4] I. Bloch, J. Dalibard, and W. Zwerger, *Many-body physics with ultracold gases*, Rev. Mod. Phys. **80**, 885 (2008).
- [5] W. Zwerger, ed., *The BCS-BEC crossover and the unitary Fermi gas*, Vol. **836** (Springer, 2011).
- [6] M. W. Zwierlein, in *Novel Superfluids*, Vol. **2**, edited by K.-H. Bennemann and J. B. Ketterson (Oxford University Press, Oxford, 2014).
- [7] I. Bloch, J. Dalibard, and S. Nascimbène, *Quantum simulations with ultracold quantum gases*, Nature Phys. **8**, 267 (2012).
- [8] M. Lewenstein, A. Sanpera, V. Ahufinger, B. Damski, A. Sen, and U. Sen, *Ultracold atomic gases in optical lattices: mimicking condensed matter physics and beyond*, Advances in Physics **56**, 243 (2007).
- [9] T. Esslinger, *Fermi-Hubbard Physics with Atoms in an Optical Lattice*, Annu. Rev. Condens. Matter Phys. **1**, 129 (2010).
- [10] T. Byrnes, P. Recher, N. Y. Kim, S. Utsunomiya, and Y. Yamamoto, *Quantum Simulator for the Hubbard Model with Long-Range Coulomb Interactions Using Surface Acoustic Waves*, Phys. Rev. Lett. **99**, 016405 (2007).
- [11] T. Byrnes, N. Y. Kim, K. Kusudo, and Y. Yamamoto, *Quantum simulation of Fermi-Hubbard models in semiconductor quantum-dot arrays*, Phys. Rev. B **78**, 075320 (2008).
- [12] S. Murmann, A. Bergschneider, V. M. Klinkhamer, G. Zürn, T. Lompe, and S. Jochim, *Two Fermions in a Double Well: Exploring a Fundamental Building Block of the Hubbard Model*, Phys. Rev. Lett. **114**, 080402 (2015).
- [13] M. Köhl, H. Moritz, T. Stöferle, K. Günter, and T. Esslinger, *Fermionic Atoms in a Three Dimensional Optical Lattice: Observing Fermi Surfaces, Dynamics, and Interactions*, Phys. Rev. Lett. **94**, 080403 (2005).
- [14] R. Jördens, N. Strohmaier, K. Günter, H. Moritz, and T. Esslinger, *A Mott insulator of fermionic atoms in an optical lattice*, Nature (London) **455**, 204 (2008).
- [15] U. Schneider, L. Hackermüller, S. Will, T. Best, I. Bloch, T. A. Costi, R.W. Helmes, D. Rasch, and A. Rosch, *Metallic and Insulating Phases of Repulsively Interacting Fermions in a 3D Optical Lattice*, Science **322**, 1520 (2008).
- [16] N. Strohmaier, Y. Takasu, K. Günter, R. Jördens, M. Köhl, H. Moritz, and T. Esslinger, *Interaction-Controlled Transport of an Ultracold Fermi Gas*, Phys. Rev. Lett. **99**, 220601 (2007).
- [17] U. Schneider, L. Hackermüller, J. P. Ronzheimer, S. Will, S. Braun, T. Best, I. Bloch, E. Demler, S. Mandt, D. Rasch, and A. Rosch, *Fermionic transport and out-of-equilibrium dynamics in a homogeneous Hubbard model with ultracold atoms*, Nature Phys. **8**, 213 (2012).
- [18] L. Jin, B. Chen, and Z. Song, *Coherent shift of localized bound pairs in the Bose-Hubbard model*, Phys. Rev. A **79**, 032108 (2009).
- [19] X. Z. Zhang, L. Jin, and Z. Song, *Self-sustained emission in semi-infinite non-Hermitian systems at the exceptional point*, Phys. Rev. A **87**, 042118 (2013).
- [20] J. Spalek, *t-J Model Then and Now: a Personal Perspective from the Pioneering Times*, Acta Physica Polonica A **111**, 409 (2007).
- [21] A. Auerbach, *Interacting Electrons and Quantum Magnetism* (Springer, New York, 1994).
- [22] M. A. Nielsen, and I. L. Chuang, *Quantum Computation and Quantum Information* (Cambridge University Press, 2002).
- [23] R. Horodecki, P. Horodecki, M. Horodecki, and K. Horodecki, *Quantum entanglement*, Rev. Mod. Phys. **81**, 865 (2009).